Dissipative tunneling of a hole from Be to the valence band of GaAs

A. Dargys and N. Žurauskienė
Semiconductor Physics Institute, A. Goštauto 11, 2600 Vilnius, Lithuania
(Received 20 January 1998; revised manuscript received 13 July 1998)

The field ionization of beryllium acceptor in molecular-beam-epitaxy-grown GaAs was investigated at low temperatures, when acoustic lattice vibrations take part in the ionization process. It has been found that acoustic phonons enhance the field ionization of beryllium, the effect being stronger the higher the lattice temperature is. Experimental results are interpreted using a hydrogenic multiphonon field-ionization model. It is shown that at $T<20$ K the acoustic-phonon-assisted acceptor–valence-band tunneling process is dominated by light mass holes and deformation-potential interaction. [S0163-1829(99)07311-7]

I. INTRODUCTION

In semiconductors the tunneling dynamics of charge carriers depends on a coupling strength between a tunneling carrier and a surrounding lattice. Investigations of the dissipative tunneling till now mainly focused on optical phonons in resonant tunneling diodes, where the initial and final states of the electron or hole participating in a tunneling are free running waves (for a review see, e.g., Ref. 1). The dissipative tunneling of charge carriers from localized to free states has been investigated to a lesser extent. Optical-phonon-assisted field ionization of deep impurities was investigated in Refs. 2–5, where it was found that inclusion of the coupling with a lattice enhances the bound-free tunneling rate by many orders.

If the lattice temperature is much lower than the characteristic optical-phonon energy, then, in the field-ionization process, acoustic lattice vibrations will predominate. First experimental results[5] showed that the influence of acoustic phonons on the tunneling dynamics is not strong. Later,[6,7] using a more refined experimental method, the importance of excited donor states in the dissipative tunneling was demonstrated. Two mechanisms, acoustic-phonon-assisted tunneling from the ground level and tunneling mediated by excited levels, were found to determine the tunneling dynamics. The effect of nonequilibrium acoustic phonons on electron tunneling in double barrier $Al_xGa_{1-x}As/GaAs$ structures was recently observed in Ref. 8.

Below, the role of acoustic phonons in the dynamics of hole tunneling from a beryllium acceptor to a GaAs valence band in micrometer-size $Al_xGa_{1-x}As/GaAs$ structures is described. The excited levels of Be acceptor in GaAs are at a large distance from the ground level. This property allows one to neglect the influence of excited beryllium states in the dissipative tunneling of holes over a relatively wide temperature range. In Sec. II we describe the samples and experimental results. In Sec. III, the experimental results are compared with theory.

II. EXPERIMENT

The samples were grown by molecular beam epitaxy on a heavily doped substrate of p^+- GaAs:Zn. After deposition of a 0.4-μm-thick buffer layer, the investigated 1.68-μm-thick p-type GaAs layer, nominally doped with 3×10^{15} cm^{-3} beryllium atoms, was grown. On the top an $Al_{0.3}Ga_{0.7}As$ barrier having 0.16-μm thickness and, finally, a 2.1-μm heavily doped (Be concentration $\approx 2.3\times10^{18}$ cm^{-3}) GaAs gate electrode were grown (see Fig. 1). The width of the barrier was large enough to preclude hole tunneling through the barrier throughout the investigated electric-field range. During measurements the substrate was soldered to the inner electrode of the coaxial sample holder, and served as a second electrode. All samples were mesa shaped, with an active area of about 0.12 mm^2. At low temperatures a positive frozen charge in the barrier was found from C-T measurements. As a result, an apparent barrier thickness, depending on the sample used, was 2–3 times wider than the physical $Al_{0.3}Ga_{0.7}As$ barrier thickness.

A linearly increasing with time voltage was applied between p^+ contacts (see the inset in the Fig. 1). The presence of an $Al_{0.3}Ga_{0.7}As$ barrier precluded the flow of Ohmic current, and allowed us to observe only the transient tunneling current superimposed on a nearly constant lattice displacement current. In Fig. 2 we plot typical shapes of the current

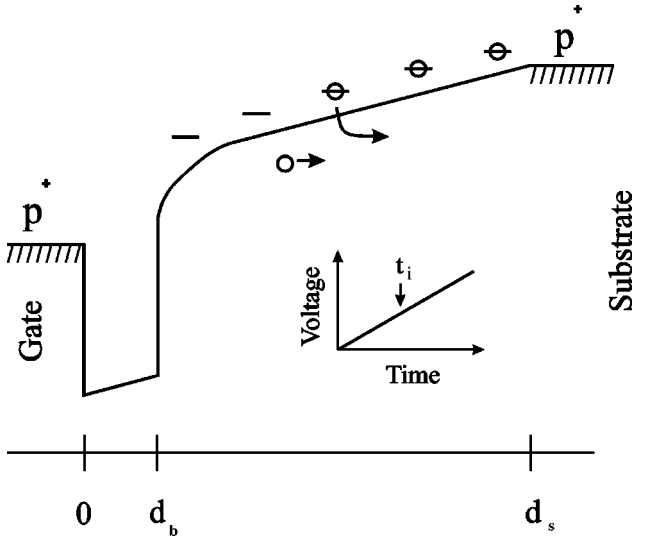

FIG. 1. A sketch of the valence-band edge and the population of Be by holes at the moment t_i, when Be field ionization just began. In the lower-right part the shape of the voltage applied between the gate and substrate is shown.

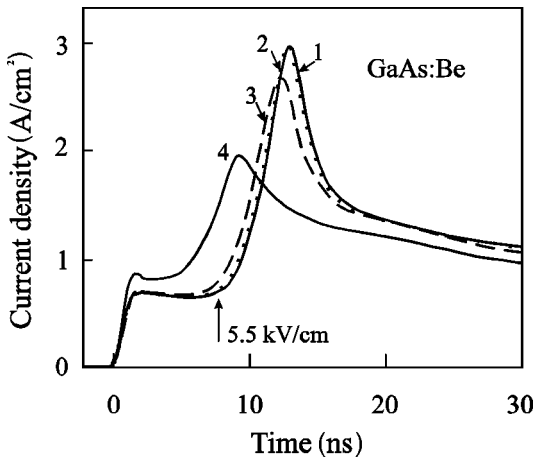

FIG. 2. The transient currents at lattice temperature: 1–4.2 K, 2–10 K, 3–15 K, and 4–25 K. The arrow indicates the moment when the electric field in the sample reached 5.5 kV/cm.

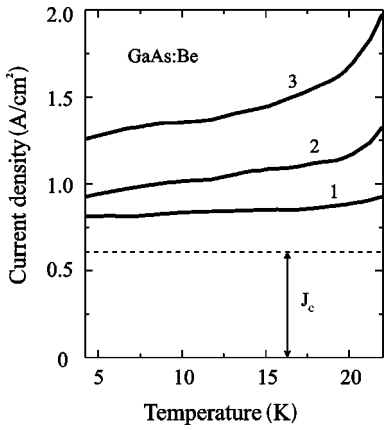

FIG. 3. Current density vs lattice temperature. The current was sampled at the moments when the electric field in the sample was 1–4.5 kV/cm, 2–4.9 kV/cm, and 3–5.5 kV/cm.

transients in an $Al_{0.3}Ga_{0.7}As/GaAs$ structure at four lattice temperatures, and at the voltage ramping rate $dV/dt=1.3\times10^8$ V/s. The moment when the electric field $F=V/d_s$ in the sample, where d_s is the distance between p^+ contacts, becomes equal to 5.5 kV/cm is indicated by the vertical arrow. At $T<20$ K all free holes are frozen on beryllium atoms, and the sample capacitance per unit area is $C=[d_b/\epsilon_b+(d_s-d_b)/\epsilon_l]^{-1}\approx6$ nF/cm^2. Here d_b and (d_s-d_b) are the barrier and GaAs layer width (cf. Fig. 1). ϵ_b and ϵ_l are the barrier and layer permittivity. The transient current in this case consists of the capacitive current and the induced current peak. The latter is due to the field ionization of beryllium atoms, and the subsequent drift of free holes to the substrate. Earlier[9,10] we observed similar transients in relatively thick ($d_s\approx10\mu$m), carbon-doped epitaxial GaAs samples having an n^+p junction instead of an $Al_xGa_{1-x}As/GaAs$ barrier. In GaAs:C samples the tunneling switched on when the electric field become larger than about 6 kV/cm. Present and previous[9,10] results show that the threshold field for effective tunneling of holes from shallow acceptors is insensitive to sample thickness and acceptor type, and is 5–6 kV/cm. We note that shallow-donor ionization in GaAs effectively begins at electric fields that are lower by an order.[10] If all acceptors were ionized, the collected charge (area under the peaks) would be equal $\frac{1}{2}eN_S=4.2\times10^{-8}$ C/cm^2, where N_S is the neutral acceptor sheet concentration in the GaAs layer. The factor $\frac{1}{2}$ takes into account the fact that the contribution of holes to the induced current depends on the acceptor coordinate with respect to the collecting electrode. For simplicity, we have neglected the finite barrier thickness. From the area under the tunneling peak one finds a somewhat smaller value: 3×10^{-8} C/cm^2. This indicates that in our samples not all acceptors are field ionized even at the highest electric fields. This is also evident from Fig. 2.

Curve 4 in Fig. 2 shows the transient current at $T=25$ K, when a small proportion of neutral beryllium atoms is thermally ionized. Now a small peak due to free thermal holes in the valence band appears at initial moments at the leading edge of the capacitive current. In general, as seen in Fig. 2, at $T<20$ K the acoustic-phonon-conditioned shift of the tunneling peak to earlier times is small.

To find the enhancement of the tunneling rate versus lattice temperature, we measured the dependence of the transient current $I(t_i)$ at some fixed moment t_i. This was achieved by changing the lattice temperature and at the same time sampling the current at the beginning of the leading edge of the tunneling peak, as shown by the arrow in Fig. 2. At the moment t_i and at $T<20$ K, only a small number of acceptors is field ionized, therefore, electric-field distortions at neutral acceptor sites due to ionization of the first acceptors is negligible. Figure 3 shows the dependence of current density $J(t_i)$ versus the lattice temperature at three moments t_i. The horizontal dashed line corresponds to the capacitive current density J_C. In all investigated samples an increase of the tunneling current density $J_t=J-J_C$, which at initial moments is proportional to the tunneling rate in the investigated GaAs layer, was observed as the lattice temperature was increased.

In Fig. 4 the points and triangles represent experimental results obtained on two 1.84-μm $Al_{0.3}Ga_{0.7}As/GaAs$ samples from the same wafer, when the sampling moments correspond to electric fields in the range $F=5$–5.6 kV/cm. The crosses were obtained with 10-μm GaAs:C sample grown earlier.[6] A range of scatter of the experimental points in Fig. 4 shows our experimental error. From Fig. 4 it is clear that the tunneling enhancement factor $R=W(T)/W(4.2)$, where $W(T)$ is the tunneling rate at temperature T, is not sensitive to acceptor type or sample length.

III. DISCUSSION

A simple theory of field ionization of a hydrogenic impurity, which neglects the complex structure of the valence band, and assumes that free hole states may be approximated by a simple parabolic band, will be used.[11] The transition energy from the ground level to the first excited level of beryllium acceptor is 16.6 meV.[12] Therefore, at lattice temperatures $T<20$ K one may safely neglect the excited level population in analyzing the tunneling dynamics. For this reason in the following we shall assume that all holes begin to tunnel from the Be ground level, and that excited Be states

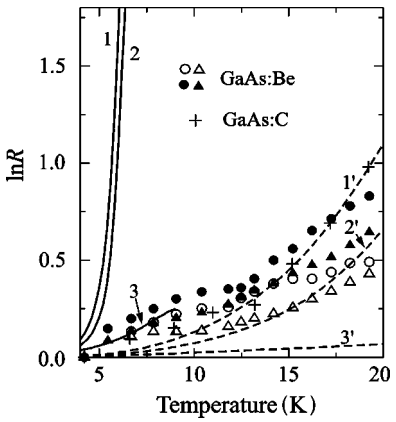

FIG. 4. Experimental (dots) and calculated (solid and dashed lines) tunneling enhancement factors due to acoustic phonons. Sample 1: $d_s=1.84$ μm; △△, $F=5.5$ kV/cm; ▲▲, $F=5.6$ kV/cm, Sample 2: $d_s=1.84$ μm; ●●, $F=5.0$ kV/cm; ○○, $F=5.5$ kV/cm, Sample 3: $d_s=10$ μm; ++, $F=6.5$ kV/cm. The curves 1 and $1'$ correspond to the cases when heavy- and light-hole masses are taken into account. Curves 2, 3 and $2',3'$ show partial contributions of, DA and PA mechanisms respectively, to 1 and $1':1=2+3$, and $1'=2'+3'$.

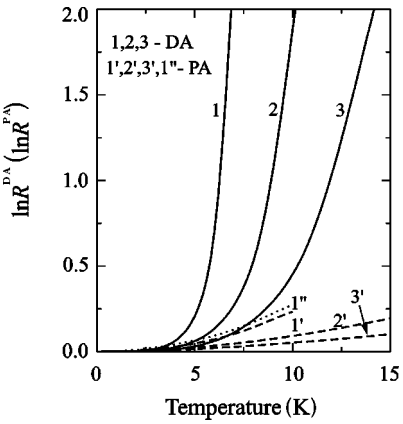

FIG. 5. Theoretical tunneling enhancement factor vs temperature for DA (solid lines) and PA (dashed lines) mechanisms at three electric-field values: $1, 1'$ –6 kV/cm, $2, 2'$ –8 kV/cm, and $3, 3'$ –10 kV/cm. The dotted line $1''$ is the PA mechanism; $q_0=0$ and $F=6$ kV/cm.

do not participate in the tunneling. According to Ref. 11 the ratio of the tunneling rates at finite and zero temperatures (the enhancement factor), due to acoustic piezoelectric (PA) and acoustic deformation-potential (DA) interaction mechanisms, is

$$R^{PA}=\exp\left[\sum_{\nu=l,t}A_{H,\nu}\int_0^{\Theta/T}dx\,\frac{Q_\nu x^3}{(x^2+x_0^2)^2(1+a_B^2q_{T,\nu}^2x^2/4)^4}\right], \tag{1}$$

$$R^{DA}=\exp\left[B_{H,l}q_{T,l}^2\int_0^{\Theta/T}dx\,\frac{Q_l x}{(1+a_B^2q_{T,l}^2x^2/4)^4}\right], \tag{2}$$

$$A_{H,\nu}=\frac{\pi\beta_{H,\nu}e^2e_{14}^2}{(2\pi)^3(\epsilon_0\epsilon_r)^2\hbar v_\nu^3\rho},\quad \beta_{H,l}=\frac{24}{35},\quad \beta_{H,t}=\frac{32}{35}, \tag{3}$$

$$B_{H,l}=4\pi E_1^2/(2\pi)^3\rho\hbar v_l^3, \tag{4}$$

$$Q_\nu=[\exp(q/q_{F,\nu})+\exp(-q/q_{F,\nu})-2]/[\exp(q/q_{T,\nu})-1]. \tag{5}$$

The subscript ν corresponds to the longitudinal ($\nu=l$) and transverse ($\nu=t$) acoustic-phonon modes with the dispersion law $\omega_\nu(q)=v_\nu q$, where v_ν is the velocity and q is the wave vector. The terms $q_{F,\nu}$ and $q_{T,\nu}$ are, respectively, field and thermal wave vectors:

$$q_{F,\nu}=\frac{eF\hbar}{2(2m^*\epsilon_i)^{1/2}\hbar v_\nu},\quad q_{T,\nu}=\frac{kT}{\hbar v_\nu}. \tag{6}$$

The integration variable in Eqs, (1) and (2) is $x=q/q_{T,\nu}$. The term $x_0=q_0/q_{T,\nu}$ takes into account the screening of the piezoelectric field, where q_0 is the inverse of the screening radius. The meaning of the other symbols is standard: e is the charge of electron or hole with a suitable sign, $\hbar$ is the Planck constant, e_{14} is the piezoelectric coefficient, ϵ_0 is the electrical constant, ϵ_r is the relative lattice permittivity, ρ is the crystal density, E_1 is the acoustic deformation potential constant, m^* is the effective mass, Θ is Debye temperature, ϵ_i is the impurity ionization energy, and a_B is the impurity Bohr radius.

The dashed and solid lines in Fig. 5 show the enhancement factors R^{PA} and R^{DA} calculated with Eqs.(1) and (2), respectively, as a function of lattice temperature in the range where the theory is valid. In these calculations the following parameter values were used[13]: $\Theta=300$ K, $E_1=8$ eV, $e_{14}=0.16$ C m^{-2}, $\epsilon_r=12.5$, $v_l=5.2\times10^5$ cm s^{-1}, $v_t=3\times10^5$ cm s^{-1}, and $\rho=5.31$ g cm^{-3}. The Bohr radius was found from $a_B=\hbar/(2m_h^*\epsilon_i)^{1/2}$, where $\epsilon_i=28$ meV is the beryllium ground-state energy. The heavy hole mass $m^*=m_h^*=0.59m_0$ was used. In accordance with Ref. 14, the influence of screening on shallow impurity field ionization was included, assuming that $q_0=0.5\times10^6$ cm^{-1}. For comparison the dots (curve $1''$) show the case when $q_0=0$, and when the electric field is 6 kV/cm. Figure 5 demonstrates that the enhancement of the hole tunneling rate is much stronger for DA interaction. In addition, the R's are larger at lower electric fields, because, at weaker fields, the localized hole can interact for a longer period of time with lattice vibrations before leaving the acceptor. However, it should be remembered that in a case of pure, i.e., without phonon participation, tunneling, the rate $W(0)$ increases with electric field [see Eq. (7)]. In other words, the rate $W(0)$ changes in the opposite direction in comparison with the enhancement factor R.

To compare between theory and experiment one has to know the quantity $R^{th}=[W^{DA}(T)+W^{PA}(T)]/[W^{DA}(4.2)+W^{PA}(4.2)]$, where W^{DA} and W^{PA} are tunneling rates for PA and DA mechanisms. As Fig. 5 shows, at $T=4.2$ K one can write approximately $W^{DA}(4.2)/W^{DA}(0)\approx1$ and $W^{PA}(4.2)/W^{PA}(0)\approx1$. Then R^{th} can be expressed through the partial enhancement factors $R^{th}\approx R^{DA}/(1+r)+R^{PA}/(1+r^{-1})$, where $r=W^{PA}(0)/W^{DA}(0)$. For a simple hydrogenic model the tunneling rates at zero lattice temperature are[11]: $W^{PA}(0)=W(0)r^{PA}$ and $W^{DA}(0)=W(0)r^{DA}$, where $W(0)$ describes the pure tunneling

$$W(0)=\frac{16\epsilon_i^2}{eF\hbar a_B}\exp\left[-\frac{4}{3}\frac{(2m^*)^{1/2}\epsilon_i^{3/2}}{eF\hbar}\right]. \quad (7)$$

The renormalization factors r^{DA} and r^{PA} are of the order of unity, and depend only weakly on lattice temperature: $r^{PA}=0.931-0.937$ in the range $T=4-13.5$ K, and $r^{DA}=0.748-0.775$ in the range $T=4-19$ K. Therefore, within our model and parameters of GaAs the ratio is $r=r^{PA}/r^{DA}=1.25-1.22$. In Fig. 4, curve 1 shows R^{th} when $r=1.23$ and $F=5.5$ kV/cm. Lines 2 and 3 indicate the partial contribution of R^{DA} and R^{PA} to 1, respectively $(1=2+3)$. It is clear, that the calculated R^{th} grows too fast compared to the experimental results if the heavy hole mass is used.

The agreement of theory with experiment can be greatly improved if one notes that at short distances from the acceptor the ground-state wave function is mainly determined by the heavy-hole mass, while at large distances the contributions from heavy- and light-hole masses are of equal importance.[15] The influence of the electric field on the tunneling enhancement mainly comes from the term $\exp[q/q_{F,\nu}]=\exp[2q(2m^*\epsilon_i)^{1/2}\hbar v/(eF\hbar)]$ in Eq. (5). It is seen that this term, apart from the electric field, also depends on the effective mass m^*. The dashed line $1'$ in Fig. 4 shows the dependence of R^{th} when in Eq. (6) m^* is replaced by a light-hole mass $m_l^*=0.0905m_0$. The lines $2'$ and $3'$ show partial contributions of DA and PA mechanisms to $1'$. Now the agreement between theory and experiment is much better. Earlier,[9,10] in accordance with the theory,[16] it has been found that a pure acceptor–valence-band tunneling dynamics is dominated by a light-mass band as well.

In conclusion, the enhancement of hole tunneling from shallow beryllium acceptors to the valence band of GaAs was observed experimentally at low temperatures, when acoustic phonons predominate in the tunneling dynamics and when excited beryllium states do not participate in the process. A satisfactory agreement between experimental results and simple theory is observed when the tunneling process is assumed to be governed by the light-hole mass, and the acceptor Bohr radius and hole binding energy by the heavy-hole mass. Of the two dissipative interaction mechanisms, deformation-potential rather than piezoelectric phonon-assisted tunneling was found to prevail. It should be stressed that in the present experiments the phonon-assisted field ionization was observed when Be was in the ground state. Earlier, using Si:P and Ge:Sb,P, we have demonstrated[6,7] that excited states may strongly influence the overall tunneling rate.

[1] H. Mizuta and T. Tanoue, *The Physics and Applications of Resonant Tunneling Diodes* (Cambridge University Press, Cambridge, 1995).

[2] Š. Kudžmauskas, Lietuvos Fiz. Rinkinys **16**, 549 (1976) [Sov. Phys. Collect. **16**, 31 (1976)].

[3] F.I. Dalidchik, Zh. Éksp. Teor. Fiz. **74**, 472 (1978) [Sov. Phys. JETP **47**, 247 (1978)].

[4] S. Makram-Ebeid and M. Lannoo, Phys. Rev. **25**, 6406 (1982)

[5] S. Žurauskas A. Dargys, and N. Žurauskienė, Phys. Status Solidi B **173**, 647 (1992).

[6] A. Dargys and N. Žurauskienė, J. Appl. Phys. **78**, 4802 (1995).

[7] N. Žurauskienė and A. Dargys, Phys. Scr. **57**, 472 (1998).

[8] F.F. Ouali, N. N. Zinov'ev, L. J. Challis, F. W. Sheard, M. Henini, D. P. Steenson, and K. R. Stickland, Phys. Rev. Lett. **75**, 308 (1995).

[9] A. Dargys, S. Žurauskas, and K. Bertulis, Phys. Status Solidi B **183**, K55 (1994).

[10] A. Dargys and S. Žurauskas, J. Phys.: Condens. Matter **7**, 2133 (1995).

[11] A. Dargys, Š. Kudžmauskas, and S. Žurauskas, J. Phys. **7**, 8967 (1995).

[12] R.A. Lewis, T.S. Cheng, M. Henini, and J.M. Chamberlain, Phys. Rev. B **53**, 12 829 (1997).

[13] A. Dargys and J. Kundrotas, *Handbook on Physical Properties of Ge, Si, GaAs, and InP* (Science and Encyclopedia Publishers, Vilnius, 1994).

[14] A. Dargys and J. Kundrotas, Phys. Status Solidi B **200**, 509 (1997).

[15] B.L. Gelmont and A.V. Rodina, Fiz. Techn. Poluprovodn. **25**, 2189 (1991) [Sov. Phys. Semicond. **25**, 1319 (1991)].

[16] H.Q. Nie and D.D. Coon, Solid-State Electron. **27**, 53 (1984).